

Lunar accretion from an impact-generated disk

Shigeru Ida^{*†}, Robin M. Canup[†] & Glen R. Stewart[†]

^{*} Department of Earth and Planetary Sciences, Tokyo Institute of Technology, Meguro-ku, Tokyo 152, Japan

[†] LASP, University of Colorado, Campus Box 392, Boulder, Colorado 80309-0392, USA

Although the mechanism by which the Moon was formed is currently unknown, several lines of evidence point to its accretion from a circumterrestrial disk of debris generated by a giant impact on the Earth. Theoretical simulations show that a single large moon can be produced from such a disk in less than a year, and establish a direct relationship between the size of the accreted moon and the initial configuration of the debris disk.

Many models have been proposed for formation of the Moon¹, but no one has succeeded in showing the formation satisfactorily. The popular “giant impact”^{2,3} model states that a Mars-sized protoplanet hit the proto-Earth and generated a circumterrestrial debris disk from which the Moon accreted. This model has been favoured as it may well account for the dynamical and geochemical characteristics of the Moon (large angular momentum of Earth–Moon system, depletion of volatiles and iron). Many hydrodynamic simulations (a smoothed particle method) have modelled the impact process^{4–7}. They calculated the impact between two large protoplanets with iron cores and silicate mantles and followed the orbital evolution of the debris after the impact for short timescales (on the order of a few orbital periods). It is found that an impact by a Mars-sized body usually results in formation of a circumterrestrial disk rather than direct formation of a clump. (This trend is most clear in recent simulations^{5–7}.) The disk mass is usually smaller than $2.5M_L$, where M_L is the present lunar mass ($0.0123M_\oplus$; M_\oplus is the Earth mass). Most of the disk material is distributed near or interior to the radius a_R of the Roche limit ($\sim 2.9R_\oplus$, where R_\oplus is the radius of the Earth) if the orbital angular momentum of the impact is $1–2J_{EM}$, where J_{EM} is the angular momentum of the present Earth/Moon system. Within and near the Roche limit, the tidal force of the Earth inhibits accretional growth.

In contrast, little has been done to simulate the accretional process of the Moon. The only published accretion calculation is that of Canup and Esposito⁸ with a gas dynamic approach. They approximated disk particles as particles in a box and tracked the evolution of the mass distribution function at individual regions of the disk, modelling velocity evolution, accretion and rebounding of

the disk particles. They showed that, in general, many small moonlets are formed initially rather than a single large moon and concluded that the simplest way to form the present-sized moon is to begin with at least a lunar mass of material outside the Roche limit. However, in gas-dynamic calculations it is difficult to include non-local effects such as radial migration of the disk material and global interaction between formed moons and the disk. The importance of the radial diffusion out from the Roche limit has been pointed out through analytical argument⁹.

Here we perform directly N -body simulations, which automatically include non-local effects, to investigate global lunar accretion processes. The sequence of accretion of the moon from an impact-generated disk might be as follows^{8,10} (see Fig. 1). Initially, the disk would probably be a hot, silicate-vapour atmosphere/torus^{6,7}. Solid particles condense owing to cooling of the disk, possibly after some radial migration¹⁰. Subsequent collisions and fragmentation of the particles would damp initially large orbital eccentricities and inclinations of the particles to moderate values in a few orbital periods. Our simulations start from this stage and follow the collisional evolution to a moon(s). On a longer timescale, one or more formed moons gradually migrate outwards by tidal interaction with the Earth^{8,10}, sweeping remnants. We do not pursue such long-term evolution here.

We present the results of 27 simulations with different initial disk conditions. We found that a single large moon, rather than multiple moons, is usually formed at similar distance from the proto-Earth in 100–1,000 orbital periods (about a month to a year). We also found that the final moon mass is mostly determined by a simple function of initial total mass and angular momentum of the disk. To estimate

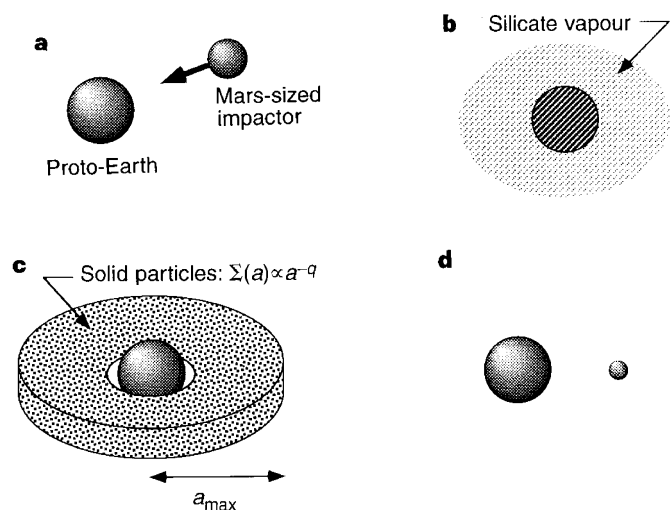


Figure 1 Schematic illustrations of the formation of the Moon by a giant impact: **a**, a Mars-sized body's impact on the proto-Earth; **b**, a hot, silicate vapour atmosphere/torus; **c**, a solid particle disk from which one or more moons accrete; **d**, outward migration of the formed moon(s) by tidal interaction with the Earth. We adopted stage **c** as the initial conditions for N -body simulations. The particle disk is modelled as follows. The disk consists of solid particles with a power-law size distribution as $n(m)dm \propto m^{-p}dm$, where m is mass of the particles. The surface density of the disk is given by $\Sigma(a) \propto a^{-q}$ for $0.35a_R < a < a_{max}$, where a is the semimajor axis. The orbits of the disk particles are integrated by a fourth-order hermitian integrator¹⁶ with a hierarchical individual time step¹⁷, calculating all gravitational interactions between the particles, in geocentric cartesian coordinates. We take out particles from the system if they collide with the Earth or are scattered into hyperbolic orbits. We adopt the accretion criteria of Canup and Esposito¹¹ (see text).

the final moon mass, we do not need to know the details of initial mass, size and velocity distributions of the disk particles. The predicted moon mass from the disks obtained by the previous impact simulations might be as large as the present lunar mass in some cases. However, we cannot make a definitive conclusion at present, as the previous impact simulations did not provide enough data about the disk angular momenta. Improved simulations are needed to provide total mass and angular momentum of the disk. The combination of more refined N -body and impact simulations would clarify whether a giant impact could indeed have produced the Moon or not.

Model description

We simulated the formation of a moon from a (three-dimensional) circumterrestrial debris disk initially consisting of 1,000–2,700 particles with mass $m \approx 10^{-5}$ to $10^{-2} M_L$ (see Fig. 1), assuming that solid particles had condensed and attained such sizes through accretion. (In the inner part of the disk, the particles might remain very small, as accretion becomes increasingly inhibited inside the Roche limit. Furthermore, the disk material might remain liquid owing to the longer cooling time in the inner part. We will comment on these effects later.)

We calculated disks with as many different initial conditions as possible, as we do not have enough knowledge about disk conditions after the vapour/liquid phase and initial collisional evolution. The parameters we examined are summarized in Table 1, where we show 19 runs of the 27 simulations for which we retained detailed output data. As shown below, the final outcome of accretion has only a weak dependence on the details of conditions of a starting disk. We scale the orbital radii by the Roche radius defined by $a_R = 2.456(\rho_{\oplus}/\rho)^{1/3} R_{\oplus}$ where (ρ_{\oplus}/ρ) is the ratio of the internal density of the Earth to that of the disk particles. For disk

particles with $\rho = 3.34 \text{ g cm}^{-3}$ (the bulk density of the Moon), a_R is located at about $2.9R_{\oplus}$. Using a_R , the physical radii of disk particles with mass m are given by $R = (1/2.456)(m/M_{\oplus})^{1/3} a_R$, independent of (ρ_{\oplus}/ρ) .

Near the Roche radius, tidal forces of the proto-Earth affect whether colliding particles rebound or accrete. Within $\sim 0.8a_R$, tidal forces preclude accretion, whereas in the transitional zone, $0.8\text{--}1.35a_R$, limited accretional growth can occur¹¹. Exterior to this zone, accretion is largely unaffected by tidal forces. This transitional zone will be referred to as the Roche zone. We adopt here the accretional criteria of Canup and Esposito¹¹, which include this transition in addition to the impact velocity condition that, for accretion, the calculated rebound velocity must be smaller than some critical value corresponding to the (mutual) surface escape velocity¹¹. If the colliding bodies in our simulation satisfy the criteria, we produce a merged body, conserving momentum. If not, the bodies rebound with given restitution coefficients (Table 1).

Characteristics of moon accretion

Below we present the results from several of the 27 disk simulations that were calculated. In most of the simulations, a single large body is formed near the Roche radius. In Figs 2 and 3, we show snapshots of the results for the disks with initial mass $M_{\text{disk}} = 0.03M_{\oplus}$ ($= 2.44M_L$). The unit of time is the keplerian rotation time at a_R , which is ~ 7 h; $t = 100$ realistically corresponds to 1 month. Figure 2 shows a centrally confined disk case (run 4 in Table 1) in which the semimajor axes of all the particles are initially within the Roche radius, whereas Fig. 3 is a rather extended disk case (run 9). The extension of a disk is indicated by $J_{\text{disk}}/M_{\text{disk}}$, where J_{disk} is the total angular momentum of the starting disk. For the disks in Figs 2 and 3, $J_{\text{disk}}/M_{\text{disk}}$ are $0.692 \sqrt{GM_{\oplus} a_R}$ and $0.813 \sqrt{GM_{\oplus} a_R}$, respectively.

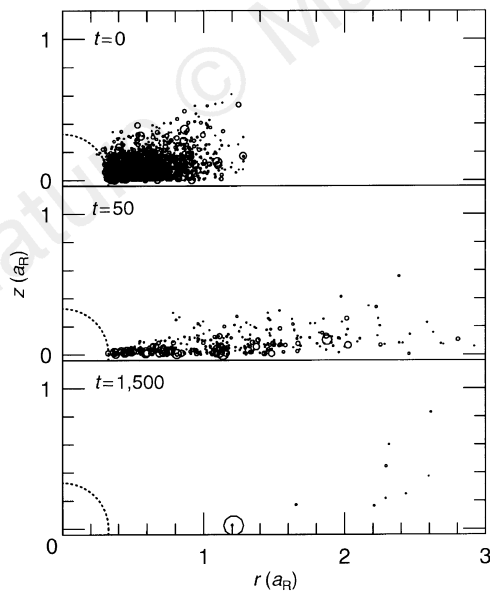


Figure 2 Snapshots of disk particles plotted in geocentric cylindrical coordinates (r, z). (Particles at negative z are plotted at $|z|$.) The units of length and time are the Roche limit radius, a_R , and Kepler time, T_{Kep} at a_R (~ 7 h). The solid and dotted circles are disk particles and the Earth, respectively. The sizes of the circles indicate physical sizes. The snapshots here are the result of run 4 in Table 1. The mean specific angular momentum, $J_{\text{disk}}/M_{\text{disk}}$, is initially $0.692 \sqrt{GM_{\oplus} a_R}$. At $t = 1,500$ the moon has mass $0.40M_L$, semimajor axis $1.20a_R$, eccentricity 0.09 and inclination (radian) 0.02. The second body's mass is only $0.025M_L$. The masses ejected from the system (M_{e}) and that hit the Earth are $0.026M_L$ and $1.95M_L$, respectively.

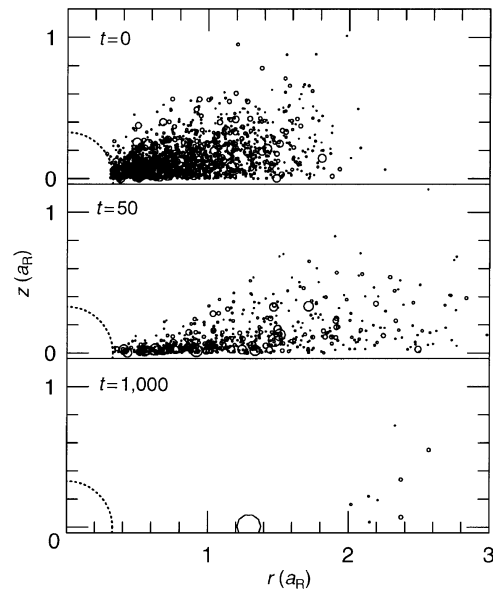


Figure 3 The same snapshots as in Fig. 2 but for run 9 of a more extended disk ($J_{\text{disk}}/M_{\text{disk}} = 0.813 \sqrt{GM_{\oplus} a_R}$). At $t = 1,000$ the largest moon mass is $0.71M_L$.

If all the disk material is at a_R , $J_{\text{disk}}/M_{\text{disk}} = \sqrt{GM_{\oplus}a_R}$. The most recent impact simulations⁷ suggest $0.6\sqrt{GM_{\oplus}a_R} \leq J_{\text{disk}} \leq 0.9\sqrt{GM_{\oplus}a_R}$ (see the last section).

The middle panels of each figure show the first stage of disk evolution where the disk shrinks in the z -direction owing to collisional damping and the disk diffuses radially by angular momentum transfer. Density waves develop in the inner region with high surface density when the disk scale height becomes so small that the disk self-gravity becomes important. The waves accelerate the angular momentum transfer and the spreading of the disk material, as expected⁹. The waves are transient (duration is only ~ 10 rotational periods) because disk materials are quickly spread out so that the disk becomes gravitationally stable again. Furthermore, as shown below, large bodies immediately form near the Roche zone and soon start to perturb the entire disk. Hence, (smooth) disk evolution as an accretion disk terminates before the disk converges to some common geometry. We found that the dominant wave patterns look like several spiral arms. The relatively large number of arms might be caused by the relatively large ratio of inner radius to outer radius of the disk (annulus) that is required by the finite radius of the Earth at the centre of the disk. However, the spiral patterns are not always clear as the number of particles in our present simulations is insufficient to resolve them accurately. As the self-gravitational instability is regulated by surface density but not by each particle size¹², the density waves would develop similarly even if we were to start with more realistic, smaller particles, whereas transfer of angular momentum associated with collisions would diminish. As the density waves have an important role in mass transfer from the Roche limit, higher-resolution N -body simulations are required for future studies.

Near or outside the Roche zone accretion starts, whereas particles remain small in the inner region because accretion is tidally inhibited inside the Roche zone (see the middle panels of Figs 2 and 3). Note that substantial mass is transferred from inside the Roche zone to start accretion, in particular, in Fig. 2. As the orbital frequency, surface density, and hence collision rate decrease with

distance from the Earth, a large body is first formed near the Roche zone (innermost region of the accretion-permitted region). The large body has relatively small velocity dispersions (eccentricity and inclination), which is due to energy equipartition through collisions and gravitational scattering¹³. This facilitates rapid growth of the large body¹³. The largest bodies have attained 90% of the final masses already at $t = 150$ and 250 in the runs in Figs 2 and 3, respectively.

The increasing gravity of the largest body eventually perturbs almost the entire disk. This can be understood from the following argument: by the balance between gravitational/collisional stirring and dissipation due to inelastic collisions, the velocity dispersion, v , of the disk particles grows to about the surface escape velocity v_{esc} of the dominant body¹⁴, which is given by $(2Gm/R)^{1/2} \approx 2(m/M_{\oplus})^{1/3}(r/a_R)^{1/2}v_{\text{Kep}}$, where r is distance from the Earth and v_{Kep} is the Kepler velocity at r . The particles in the width $\Delta r \approx 2er \approx 2vr/v_{\text{Kep}}$ cross the large moon's orbit. Substituting $m \approx M_L$ and $r \approx a_R$, we find $\Delta r \approx a_R$. Hence, unless the disk is substantially extended or the final moon mass is much smaller than M_L , the entire disk is perturbed by the largest body's gravity, so that the other disk particles are 'cleaned up' (scattered onto the Earth or into hyperbolic orbits or accreted by the largest body). Thereby a single moon on a nearly circular orbit remains near the Roche zone as is shown in the bottom panels of Figs 2 and 3.

The other calculations with different initial conditions show a quite similar outcome, as long as an initial disk is not very extended: a single large moon on a nearly circular orbit. The final position of the large moon is $0.9-1.6a_R$ ($2.6-4.6R_{\oplus}$). The variety of the final position is caused by recoil of the 'clean-up'. If tidal interaction with the Earth were included, the formed moon would gradually migrate outward on a much longer timescale, presumably sweeping up any remaining smaller outer debris^{8,10}. (Inner remaining bodies within $0.7-0.8a_R$ (co-rotation radius) would gradually migrate to the Earth⁸.)

Figure 4 shows the evolution of a very extended disk ($J_{\text{disk}}/M_{\text{disk}} = 0.985\sqrt{GM_{\oplus}a_R}$; run 13) where the disk width is

Table 1 Input parameters and results of the simulations

| $M_{\text{disk}} = 2.44; \rho = 1.5$ | | | | | | | | | | | | | |
|--------------------------------------|-----------------------------------|-------------------|-------------------|--------|-------|--------------|------|--------|-------|--------------|-------|-------|--------------|
| Run | $J_{\text{disk}}/M_{\text{disk}}$ | J_{disk} | a_{max} | q | N | ϵ_n | a | M | M' | M_{∞} | J | J' | J_{∞} |
| 1 | 0.670 | 0.300 | 0.95 | 5 | 1,500 | 0.01 | 1.08 | 0.193* | 0.356 | 0.010 | 0.036 | 0.084 | 0.001 |
| 2 | 0.670 | 0.300 | 0.95 | 5 | 1,500 | 0.5 | 1.69 | 0.216* | 0.248 | 0.065 | 0.051 | 0.060 | 0.017 |
| 3 | 0.690 | 0.308 | 0.95 | 4 | 1,000 | 0.01 | 0.87 | 0.252 | 0.437 | 0.016 | 0.043 | 0.094 | 0.007 |
| 4 | 0.692 | 0.309 | 0.95 | 4 | 2,000 | 0.01 | 1.20 | 0.400 | 0.464 | 0.026 | 0.080 | 0.099 | 0.005 |
| 5 | 0.722 | 0.323 | 1.25 | 3 | 1,000 | 0.01 | 0.88 | 0.437 | 0.484 | 0.109 | 0.074 | 0.087 | 0.044 |
| 6 | 0.722 | 0.323 | 1.25 | 3 | 1,000 | 0.5 | 1.32 | 0.281 | 0.391 | 0.153 | 0.059 | 0.090 | 0.037 |
| 7 | 0.767 | 0.343 | 1.25 | 3 | 1,500 | 0.01 | 1.55 | 0.315 | 0.411 | 0.0005 | 0.070 | 0.100 | 0.0001 |
| 8 | 0.794 | 0.355 | 1.25 | 3 | 2,700 | 0.01 | 1.21 | 0.751 | 0.776 | 0.006 | 0.151 | 0.159 | 0.002 |
| 9 | 0.813 | 0.363 | 1.50 | 2 | 1,500 | 0.01 | 1.24 | 0.712 | 0.744 | 0.016 | 0.144 | 0.154 | 0.031 |
| 10 | 0.823 | 0.363 | 1.50 | 2 | 1,000 | 0.5 | 0.79 | 0.260* | 0.636 | 0.178 | 0.042 | 0.151 | 0.046 |
| 11 | 0.834 | 0.373 | 1.80 | 2 | 1,000 | 0.01 | 1.24 | 0.666 | 0.721 | 0.212 | 0.135 | 0.151 | 0.079 |
| 12 | 0.891 | 0.398 | 2.00 | 2 | 1,000 | 0.01 | 1.87 | 0.572* | 0.609 | 0.140 | 0.142 | 0.155 | 0.041 |
| 13 | 0.958 | 0.428 | 2.00 | 1 | 1,000 | 0.01 | 1.98 | 0.631* | 0.646 | 0.198 | 0.162 | 0.226 | 0.040 |
| 14 | 0.977 | 0.437 | 2.00 | 1 | 1,000 | 0.01 | 1.12 | 1.046 | 1.122 | 0.299 | 0.203 | 0.225 | 0.099 |
| $a_{\text{max}} = 1.25; q = 3$ | | | | | | | | | | | | | |
| Run | $J_{\text{disk}}/M_{\text{disk}}$ | J_{disk} | M_{disk} | ρ | N | ϵ_n | a | M | M' | M_{∞} | J | J' | J_{∞} |
| 15 | 0.738 | 0.323 | 2.44 | 0.5 | 1,000 | 0.01 | 0.93 | 0.505 | 0.685 | 0.120 | 0.089 | 0.141 | 0.040 |
| 16 | 0.757 | 0.451 | 3.24 | 1.5 | 1,000 | 0.5 | 1.19 | 0.536 | 0.631 | 0.287 | 0.107 | 0.132 | 0.075 |
| 17 | 0.767 | 0.457 | 3.24 | 1.5 | 1,500 | 0.01 | 1.45 | 0.657 | 0.694 | 0.088 | 0.142 | 0.153 | 0.031 |
| 18 | 0.768 | 0.344 | 2.44 | 1.0 | 1,000 | 0.01 | 1.53 | 0.515 | 0.668 | 0.008 | 0.117 | 0.153 | 0.003 |
| 19 | 0.778 | 0.232 | 1.62 | 1.5 | 1,000 | 0.01 | 0.91 | 0.251* | 0.444 | 0.001 | 0.044 | 0.096 | 0.004 |

Input parameters and output data of 19 runs of the 27 simulations for which we retained detailed output data. Snapshots of runs 4, 9 and 13 are shown in Figs 2, 3 and 4, respectively. Input parameters are $J_{\text{disk}}, M_{\text{disk}}, q, \rho, N$ and ϵ_n , which are angular momentum, mass and outer edge of an initial disk, power indices of surface density distribution ($\Sigma(a) \propto a^{-q}$, where a is the semimajor axis of the disk particles) and size distribution ($n(m) \propto m^{-p}$, where m is the mass of the particles), total number of disk particles and restitution coefficient in the normal direction, respectively. Units of angular momentum, mass and distance are the present angular momentum of the Earth/Moon system ($V_{\text{EM}} = 3.5 \times 10^{31} \text{ g cm}^2 \text{ s}^{-1}$), the present lunar mass M_L and the Roche radius ($a_R = 2.9R_{\oplus}$), respectively. As $M_L = 0.0123M_{\oplus}$, $M_{\text{disk}} = 1.62, 2.44$ and 3.24 correspond to $0.02M_{\oplus}, 0.03M_{\oplus}$ and $0.04M_{\oplus}$, respectively. The second column, $J_{\text{disk}}/M_{\text{disk}}$, is the specific angular momentum of the disk in units of $\sqrt{GM_{\oplus}a_R}$ (not V_{EM}/M_L). The normal restitution coefficient, ϵ_n , is set to be a constant, 0.01 or 0.5, except for collisions with very small velocity, where ϵ_n approaches unity. The tangential restitution coefficient, ϵ_t , is fixed at unity. (The non-slip case with inclusion of particle spins is a subject for future research.) Note that for even $\epsilon_n = 0.01$, collisions are not very dissipative. In most cases, initial eccentricities and inclinations (radian) of the disk particles are given by a Rayleigh distribution with a mean value of 0.3. (Different initial mean eccentricity and inclination do not change the results.) Columns 8 to 14 are output data. M and J are the mass and orbital angular momentum of the largest moon (a is its semimajor axis). M' and J' are the same quantities but including all bound debris outside the largest moon's orbit, which might finally accrete to the largest moon through tidal orbital migration. The same quantities for ejected particles are M_{∞} and J_{∞} . In column 9 (M), cases where the second body is larger than 30% of the largest body are indicated by an asterisk.

larger than $2a_R$. As expected from the above discussion ($\Delta r \approx a_R$), two large moons are formed in this case. We found that for $J_{\text{disk}}/M_{\text{disk}} \geq 0.85 \sqrt{GM_{\oplus} a_R}$, multiple moons are more common (see Fig. 5). The variety in final positions of the large moon is larger ($0.8\text{--}2.0a_R$) owing to interaction between multiple large moons. In these very extended disk cases it would be important to study the coalescence mechanism of the large moons during the subsequent tidal orbital migration, as discussed by Canup and Esposito⁸.

The accretion timescale and final mass of the moon depend on initial conditions. For a large restitution coefficient and a centrally confined disk, the accretion time is long because accretion is not favoured by the collisions with a large coefficient or those in inner regions. The final mass is in general larger in more extended disks as suggested by Figs 2 and 3 ($0.50M_L$ in Fig. 2 but $0.71M_L$ in Fig. 3). We next consider what determines the final mass.

Before that, we comment on effects of liquidity of the disk particles. In inner disk regions a hot environment might be maintained^{16,7,10}, so that disk materials might be liquid (or possibly vapour). Furthermore, energy release during collisions might melt the disk particles. During collisions the kinetic energy of relative motion is translated into heat energy. The specific dissipative energy would be $\sim e^2 v_{\text{kep}}^2 \approx 200(e/1.0)^2 (r/a_R)$ (J g^{-1}), which corresponds to a temperature increase of $\sim 200(e/0.1)^2 (r/a_R)$ K. As small particles tend to have large eccentricities (>0.3) as a result of the energy equipartition, they can melt totally during one collision (melting temperature of silicate is 1,200–1,300 K). Such melting might lead to tidal disruption of the particles inside the Roche zone to form a fluid disk. Then the fluid ‘blobs’ might be in a thick vapour or in a thick swarm of other ‘blobs’ so that drag from the vapour or very inelastic collisions with the other ‘blobs’ would prevent their eccentricities from getting too high, which might affect the ‘clean-up’ process. However, the tidal torque exerted by the moon would push the inner disk to the Earth even if the eccentricities of the ‘blobs’ were damped. The moon has strong resonant interactions (2:1, 3:2, 4:3, ...) with the disk in the region of $\geq 0.6a$, where a is the semimajor axis of the Moon, and the disk in the region can easily be cleared, even if the disk is composed of gas¹⁵. This suggests that the tidal torque of the moon at $\sim a_R$ might be able to push the disk material on to the Earth surface ($0.34a_R$), or at least to well inside the co-rotation radius at $0.7\text{--}0.8a_R$ (the material inside the co-rotation radius would migrate inward by tidal interaction with the Earth). Thus, the melting of the disk particles would not affect the ‘clean-up’ process we showed, although the timescale to accomplish it might become longer.

Mass of the moon

On the basis of the result obtained by N -body simulations, we can derive a simple formula to obtain the largest moon’s mass. It is a function of only two parameters: initial disk mass, M_{disk} , and angular momentum, J_{disk} . Conservation of angular momentum gives

$$J_{\text{disk}} \approx M \sqrt{GM_{\oplus}(1-e_1^2)a_1} + (M_{\text{disk}} - M - M_{\infty}) \sqrt{GM_{\oplus}(1-e_2^2)a_2} + M_{\infty} \sqrt{GM_{\oplus}(1-e_3^2)a_3} \quad (1)$$

where M , $(M_{\text{disk}} - M - M_{\infty})$ and M_{∞} are the masses of the largest moon, mass accreted to the Earth and ejected mass, respectively, and e_k , a_k and $\sqrt{GM_{\oplus}(1-e_k^2)a_k}$ ($k = 1, 2, 3$) are their orbital eccentricities, semimajor axes and specific angular momenta. Here we assumed that the total mass of remnant small bodies is negligible. The perigee distance $(1-e_3)a_3$ is $\sim a_1$, as the escaping bodies are usually scattered by the largest moon. In contrast, $(1-e_2)a_2 \leq R_{\oplus}$ ($\sim 0.34a_R$); we take $(1-e_2)a_2 \approx 0.3a_R$. From our simulations we find typical values of: $e_1 < 0.1$, $a_1 \approx 1.3a_R$, $e_2 \approx 0.2\text{--}0.3$ and $e_3 \approx 1$. Substituting these into

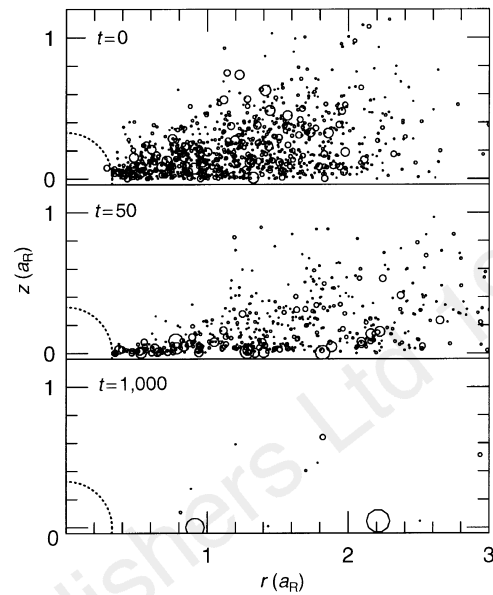


Figure 4 The same snapshots as in Fig. 2 but for run 13 of a very extended disk ($U_{\text{disk}}/M_{\text{disk}} = 0.958 \sqrt{GM_{\oplus} a_R}$). In this case two large moons are formed. At $t = 1,000$ the largest moon has mass $0.63M_L$ and semimajor axis $1.98a_R$, whereas the second has $0.39M_L$ and $0.93a_R$.

equation (1), we obtain

$$M \approx \frac{1.9J_{\text{disk}}}{\sqrt{GM_{\oplus} a_R}} - 1.15M_{\text{disk}} - 1.9M_{\infty} \quad (2)$$

Ejected mass M_{∞} is negligible in confined disks with small $J_{\text{disk}}/M_{\text{disk}}$ ($M_{\infty} \leq 0.05M_{\text{disk}}$ for $J_{\text{disk}}/M_{\text{disk}} \leq 0.8 \sqrt{GM_{\oplus} a_R}$), whereas it often takes a large value for more extended disks. The simulations with larger $J_{\text{disk}}/M_{\text{disk}}$ eject more material out of Earth orbit because disk material in shallow potential of the Earth (in the outer part) can easily be ejected and because gravitational interactions with multiple moons are more effective at pumping up the energy of the smaller particles. The ejected mass also tends to take a large value when the restitution coefficient is large.

In Fig. 5 we compare equation (2) (with both sides divided by M_{disk}) with N -body simulation results. The final moon mass in the N -body simulations is the value at which the residual disk mass becomes sufficiently small compared with the moon mass or disk evolution becomes very slow (usually at $t = 500\text{--}2,000$ rotational periods). The simulation results include large varieties of initial disk conditions, final moon masses and restitution coefficient. The lines of equation (2) with $M_{\infty} = 0$ and $0.05M_{\text{disk}}$ are drawn. For $J_{\text{disk}}/M_{\text{disk}} \leq 0.8 \sqrt{GM_{\oplus} a_R}$, the simulation results are consistent with the theoretical lines with small M_{∞} . The theoretical estimate would exhibit a smaller slope and would become more consistent with the simulation results if we allowed M_{∞} to increase systematically with $J_{\text{disk}}/M_{\text{disk}}$ as mentioned above. Larger M_{∞} inhibits the formation of a large moon, as much more mass than M_{∞} falls on to the Earth to compensate the angular momentum loss.

For disks with $J_{\text{disk}}/M_{\text{disk}} \leq 0.8 \sqrt{GM_{\oplus} a_R}$, which would in practice be important, the third term in the right-hand side of equation (2) is usually small compared with the other terms (if we adopt a non-slip rebounding condition, $e_1 < 1$, M_{∞} might become smaller). Therefore, we conclude that the final moon mass is determined mostly by two parameters, J_{disk} and M_{disk} , but not by the other detailed initial conditions or rebounding conditions (their effects are included in a small correction term, M_{∞}). This conclusion allows

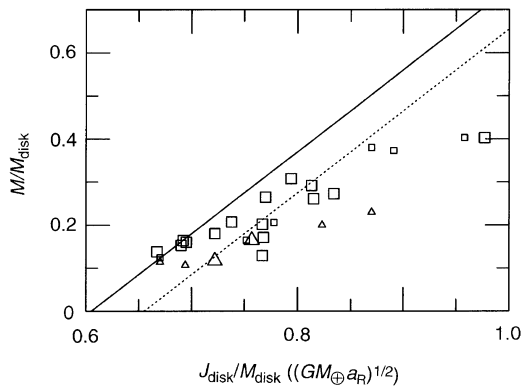


Figure 5 Final moon mass, M , is plotted on the $M/M_{\text{disk}} - J_{\text{disk}}/M_{\text{disk}}$ plane. Smaller $J_{\text{disk}}/M_{\text{disk}}$ cases are confined disks with smaller a_{max} and larger q . The solid line is the analytical estimate by equation (2) with $M_{\infty} = 0$; the dotted line is that with $M_{\infty} = 0.05M_{\text{disk}}$. Squares are N -body results with $\epsilon_n = 0.01$ and triangles are N -body results with $\epsilon_n = 0.5$. The small squares and triangles are the cases where the mass of a second moon is larger than 30% of the largest moon's mass. In these cases we plotted the sum of the largest and second moons' masses. Here we plotted the results of all 27 simulations.

us to predict easily the outcome of the complicated accretion process in the protolunar disk.

Application to the results of previous impact simulations

From the above results we estimate the expected moon masses that would result from the impact-generated disks obtained by previous hydrodynamic simulations. Unfortunately, the previous impact simulations⁴⁻⁷ did not present J_{disk} , although M_{disk} was presented in many cases. Here we roughly estimated J_{disk} from the published data^{4,5}: surface density histograms⁴ and a table of the initial disk masses within and exterior to the Roche limit⁵. The estimated $J_{\text{disk}}/M_{\text{disk}}$ is distributed from $0.7\sqrt{GM_{\oplus}a_R}$ to $1.1\sqrt{GM_{\oplus}a_R}$, although our estimates include a large uncertainty. Figure 4 suggests that $M/M_{\text{disk}} = 0.15-0.4$ for such $J_{\text{disk}}/M_{\text{disk}}$. Because the disks produced by the previous impact simulations have $M \leq 2.5M_L$, it seems possible for some disks to yield a lunar-sized moon. However, results of recent higher-resolution simulations⁷ ($1M_L$ is represented by ~ 300 smoothed particles) suggest that the resolution of the previous works ($1M_L \approx 37$ particles) might not have been adequate to describe the initial disk mass distribution. The higher-resolution disks generated tend to be more centrally confined and, equivalently, to have smaller $J_{\text{disk}}/M_{\text{disk}}$ (presumably, $J_{\text{disk}}/M_{\text{disk}} \approx 0.6-0.9\sqrt{GM_{\oplus}a_R}$ for impacts of $\leq 2J_{\text{EM}}$), although the higher-resolution simulations⁷ did not provide specific data about J_{disk} and M_{disk} . In this case we would predict a smaller final moon mass for similar M_{disk} .

In general, impacts with higher angular momentum produce more massive and extended disks⁴⁻⁶ that provide more material outside the Roche zone. We can predict the formation of a moon

with at least a lunar mass from most of the disks produced by the impacts with $\geq 2J_{\text{EM}}$, for relatively small M_{∞} . However, no reasonable means to rid the Earth/Moon system of this excess angular momentum has yet been proposed. This problem was pointed out by Canup and Esposito⁸. Furthermore, the present N -body simulations show that accretion from an extended disk often results in large M_{∞} , which inhibits the formation of a large moon as mentioned above and usually produces multiple moons, where we are faced with another problem on the coalescence of the multiple moons⁸.

In this work we have identified a direct relation between the initial mean specific angular momentum of a disk and the fraction of the disk mass that eventually becomes incorporated into the single large resulting moon. This result gives an important clue to the problem of the Moon formation (although more detailed N -body simulations might be needed to examine wider disk parameter ranges with more realistic, smaller starting particles). Improved impact simulations are needed to provide more detailed initial disk conditions, in particular J_{disk} and M_{disk} . Furthermore, angular momentum and mass transport might be important during the evolution from the initial vapour state to a particulate disk¹⁰. This problem should be addressed by some new fluid-dynamical simulations (or fluid/particles hybrid simulations). The combination of these simulations with different approaches is needed to clarify the formation of the Moon. □

Received 21 March; accepted 1 August 1997.

1. Boss, A. P. & Peale, S. J. in *Origin of the Moon* (eds Hartmann, W. K., Phillips, R. J. & Taylor, G. J.) 59-102 (Lunar and Planetary Inst., Houston, 1984).
2. Hartmann, W. K. & Davis, D. R. Satellite-sized planetesimals and lunar origin. *Icarus* **24**, 504-515 (1975).
3. Cameron, A. G. W. & Ward, W. R. The origin of the Moon. *Proc. Lunar Planet Sci. Conf.* **7**, 120-122 (1976).
4. Benz, W., Slattery, W. L. & Cameron, A. G. W. The origin of the Moon and the single impact hypothesis. I. *Icarus* **66**, 515-535 (1986).
5. Benz, W., Cameron, A. G. W. & Melosh, H. J. The origin of the Moon and the single impact hypothesis. III. *Icarus* **81**, 113-131 (1989).
6. Cameron, A. G. W. & Benz, W. The origin of the Moon and the single impact hypothesis. IV. *Icarus* **92**, 204-216 (1991).
7. Cameron, A. G. W. The origin of the moon and the single impact hypothesis. V. *Icarus* **126**, 126-137 (1997).
8. Canup, R. M. & Esposito, L. W. Accretion of the Moon from an impact-generated disk. *Icarus* **119**, 427-446 (1996).
9. Ward, W. R. & Cameron, A. G. W. Disc evolution within the Roche limit. *Proc. Lunar Planet Sci. Conf.* **9**, 1205-1207 (1978).
10. Stevenson, D. J. Origin of the moon—the collision hypothesis. *Annu. Rev. Earth Planet. Sci.* **15**, 271-315 (1987).
11. Canup, R. M. & Esposito, L. W. Accretion in the Roche zone: co-existence of rings and ringmoons. *Icarus* **113**, 331-352 (1995).
12. Goldreich, P. & Tremaine, S. The dynamics of planetary rings. *Annu. Rev. Astron. Astrophys.* **20**, 249-248 (1982).
13. Stewart, G. R. & Wetherill, G. W. Evolution of planetesimal velocities. *Icarus* **74**, 542-553 (1988).
14. Safronov, V. S. *Evolution of the Protoplanetary Cloud and Formation of the Earth and Planets*. (Nauka, Moscow, 1969).
15. Lin, D. N. C. & Papaloizou, J. C. B. in *Protostars and Planets III* (eds Levy, E. H. and Lunine, J. I.) 749-836 (Univ. Arizona Press, Tucson, 1993).
16. Makino, J. & Aarseth, S. J. On a Hermite integrator with Ahmad-Cohen scheme for gravitational many-body problems. *Publ. Astron. Soc. Jpn* **44**, 141-151 (1992).
17. Makino, J. A modified Aarseth code for GRAPE and vector processors. *Publ. Astron. Soc. Jpn* **43**, 859-876 (1991).

Acknowledgements. We thank A. G. W. Cameron and Jack Lissauer for their constructive criticisms, and W. Ward, L. Esposito and H. Tanaka for discussions and comments. S.I. thanks LASP, University of Colorado for hospitality. R.M.C. was supported by NASA's origins of solar systems programme, and G.R.S. was supported by NASA's planetary geology and geophysics programme.

Correspondence and requests for materials should be addressed to S.I. (e-mail: ida@geo.titech.ac.jp).